CLAS-NOTE 2004-016

Measurements of PMT time resolution at Kyungpook National University.

Status report

V.N.Batourine, W.Kim,
D.M.Nekrasov, K.Park, B.Shin,
E.S.Smith, S.S.Stepanyan.

May 5, 2004

Introduction

The barrel "time zero" detector of CLAS is formed by 56 scintillating counters 50cm long and $2.3 \times 3cm^2$ in section. These counters are located 25cm apart the beam. One of the challenges of the ongoing upgrade of the CLAS TOF system is to provide the TOF resolution of about 50ps.

The timing information in CLAS has been taken from both ends of extended scintillators. In such a case theTOF resolution is close to a standard deviation of a PMT timing σ_{PMT}(assuming identical resolution of all PMTs).

Hence, the main goal of our studies at KNU is to develop a prototype for the time-zero counter providing the effective resolution $\sigma_{PMT} \approx 50ps$. We call σ_{PMT} as "effective resolution" in order to emphasize that this value is defined not only by the excellent characteristics of PMTs, which we use in our studies. Below we discuss several approaches for measuring σ_{PMT}.

Plans and Accomplishments. Year 2003.

The goal for this year was to achieve σ_{PMT} as close as possible to the desired value with the simplest counter prototype. For understanding the performance of the detector at such a challenging level a profound multi-parameter analysis is required. The input for such analysis has to include both the timing and amplitude information from PMTs.

With this purposes in mind the plan of KNU group for the Year 2003 was the following.

- To make the prototype for CLAS timing counter.
- To produce the assembly of 3 identical counters.
- To develop the Data Acquisition system in both CAMAC and VME standards.
- To perform various test and to collect data with radiative source and cosmic rays,as well

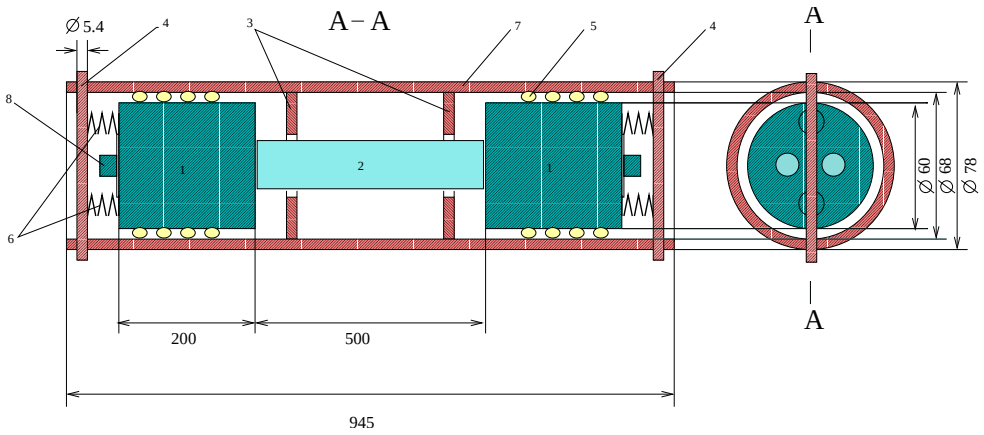

Figure 1: Counter design-1. (1)-PMTs, (2) - scintillator,(3)-supporting "o"-rings, (4)-studs,(5)-condensing rings,(6)-springs,(7)-plastic tube,(8)- connectors

0.1 Scintillation counters.

Counter design-1. No light guides. We began our studies of the PMT resolution with the counter shown in Fig.1. The counter is manufactured with a plastic scintillator "BICRON 408", sized as $20 \times 33 \times 500\ mm^3$. Two PMTs R2083 of "Hamamatsu Corporation" are attached directly to the scintillator. Thus, the scintillations has been viewed from both ends. R2083 has an excellent rise time of about $0.7ns$ and transition time of about $16ns$. The diameter of its cathode is of $52 \pm 1mm$. The upper limit of the HV is of about 3kV.

This simplest design provides a maximum possible light signal on the cathode. From tests with such counters we expect to obtain the lower limit for σ_{PMT}.

Counter design-2. Long light guides. The next logical step would be a counter with 1m long light guides(see Fig.2). We plan to produce a triplet of such counters in 2004. We intend to investigate its performance after we'll do our best to improve σ_{PMT} yielding from the Design-1.

Long air light guides provide quite poor light collection. Thus, from this design we'll obtain the upper limit for σ_{PMT}. For a future we plan to have made and studied a more realistic prototype with long plastic light guides.

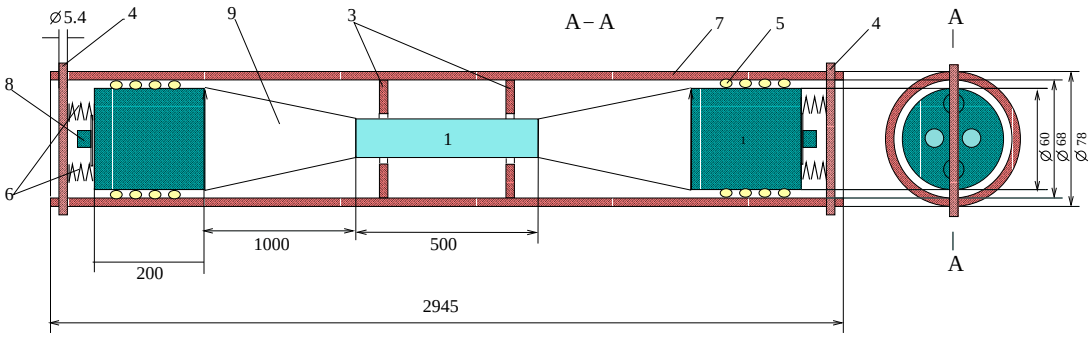

Figure 2: Counter design-2.(1)-PMTs, (2) - scintillator,(3)-supporting "o"-rings, (4)-studs,(5)-condensing rings,(6)-springs,(7)-plastic tube ,(8)- connectors, (9)-light guides.

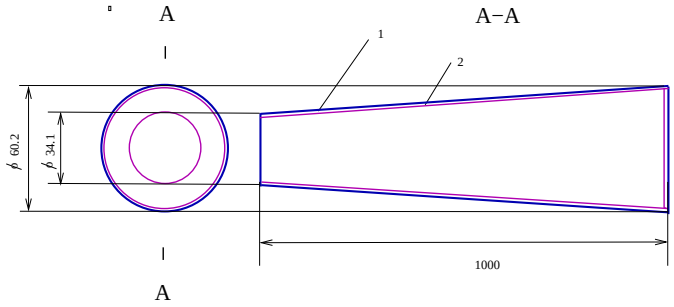

Figure 3: Conical light guide.

Light guide. The simplest possible design of the conic air light guide is shown in Fig.3. This $1m$ long air light guide is fabricated from two layers. Its inner reflecting layer is made of mylar 100μm thick. The outer layer, which provides the mechanical stability, is made of plastic 300μm thick.The reflecting lier is glued to the inner surface of the cone.

The diameter of the narrow end is equal to the diagonal of the scintillator plus $1mm$. The inner diameter of the wide end is equal to the diameter of the R2083 cathode.

The artist view of the light guides is shown in Fig.4

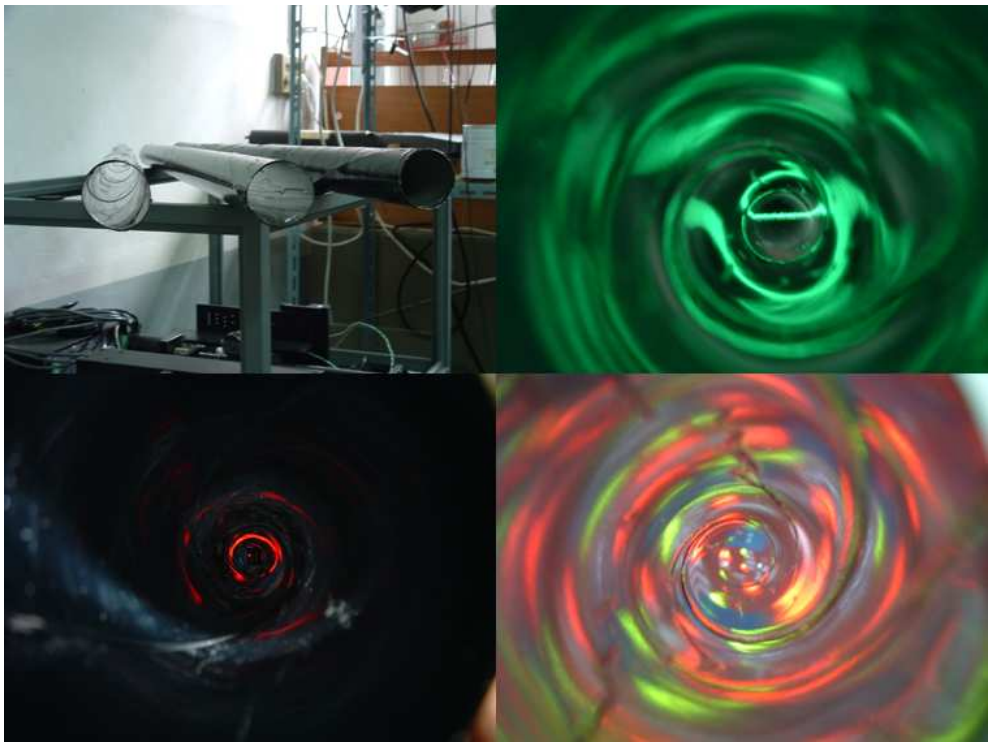

Figure 4: Artist view of the light guide.

0.2 Setup of three counters for cosmic ray tests.

An artist view of the current setup of three counters under cosmic tests is shown in Fig.5. Each of three long barrels, labeled as S1, S2 and S3, contain 2 PMTs and scintillator. Such counter may be reassembled in 5 minutes. The distance between counters is of $7.5cm$.

In order to make it possible to place the ^{90}Sr source on the surface of the scintillator, three holes were machined in each barrel: the central hole and two at $\pm 15cm$ from the middle.

.

0.3 Data acquisition.

The operating CAMAC and VME Data Acquisition Systems are also shown in Fig.5. The CAMAC based DAQ utilize the "MULTI-X" program, while the VME based DAQ utilize the "LabView" software. Two on-line spectra yielded by these DAQs can be seen on the monitor. In principle, both DAQs can run in parallel.

Our first DAQ system was developed for CAMAC standard. Most of tests

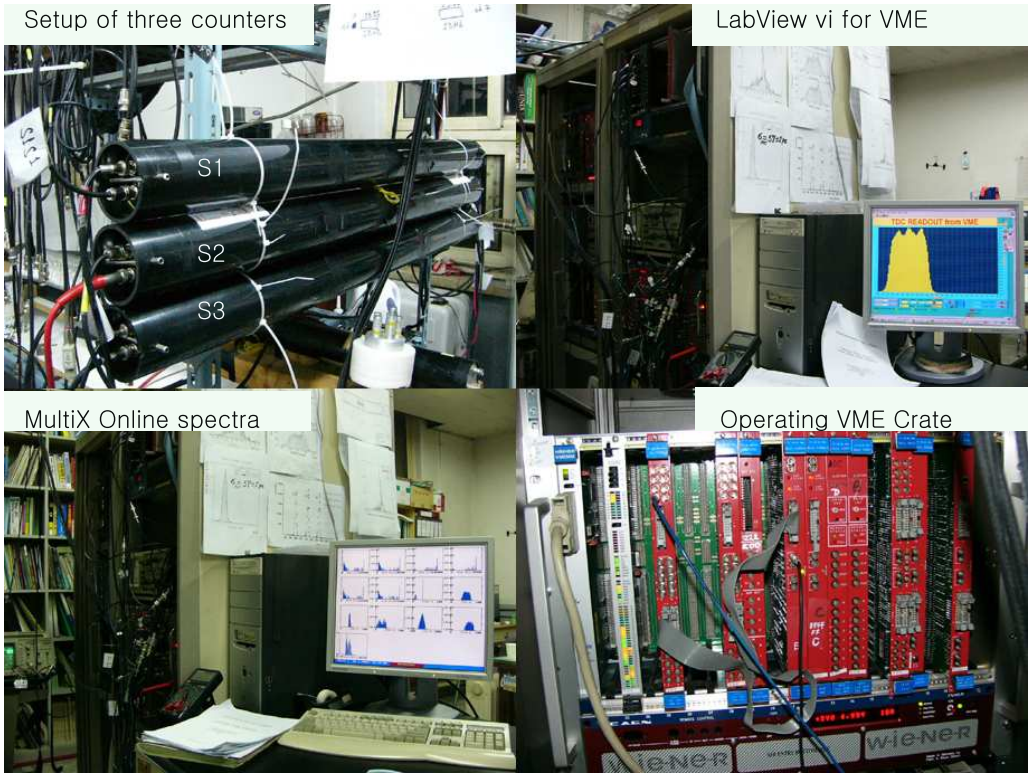

Figure 5: Artist view of the setup.

with radiation source and cosmic rays were performed with this DAQ. The schematic view of the setup of three counters together with the electronic circuit diagram is shown in Fig.6.

The hardware part of this system includes two NIM crates and one CAMAC crate instrumented with CC16 controller of WIENER. The NIM crate contains various service modules and discriminators. To discriminate signals from PMTs we use two kinds of discriminators: (1)threshold discriminators CAEN N413A and (2)constant fraction discriminator ORTEC-93.

Signals from "up"(S1) and "down"(S3) counter have been shaped by the constant fraction discriminators ORTEC-935, while for the middle counter the threshold discriminators CAEN-N413A have been used. Shaped signals have been forwarded to the inputs of TDCs(LeCroy 2228A). The common "start" has been taken from the left PMT of the "up" counter(S1), which has a 4m shorter signal cable. Therefore, all "stop"s have been arrived to the TDC after the "common start".

Thus, the arrival times $t_{i=1,..,6}$ of six PMT signals have been digitized by the LeCroy-2228A TDC.

The common "start" has been also used as ADC "gate". The width of

this signal is set to $200ns$. The corresponding charges, i.e. time integrated currents, $a_{i=1,...,6}$ has been digitized by the LeCroy-2228A ADC.

By the end of digitizing the proper "Look-At-Me" has been asserted by TDC.

The LAM status of the TDC has been permanently polled by the "Multi-X" program. The event readout has been started by LAM is "true". In order to provide the readout sequence be initialized on the coincidence of "up" and "down" counters, the dedicated NIM logical scheme was assembled. This logics utilize the "clear" inputs of both TDC and ADC to control the readout request in a following way.

The output signals from the discriminators of "up and "down"-counters has been fed to the coincidence logical unit(LeCroy-365AL). The output signal from this unit has been re-shaped by the Gate Generator(ORTEC-416A) to form the signal of appropriate width and delay. This signal has been used as a "veto" for the "or"-unit(CAEN N455), which also receives the "pro-to-clear" signal. The last has been produced in advance, with the appropriate delay and width, by the second Gate Generator(ORTEC-416A), in response to the "common start" signal.

Therefore, in case of no coincidence happened between "up" and "down" counters , the LAM signal has been cleared. Thus, the readout sequence has been generated by coincidence of "up" and "down" counters. The advantage of this approach is that we have avoided implementation of 12 long delays, which were required to fit all signals into both the ADC gate and TDC scale, as well.

The events containing 25 CAMAC words(8 TDC inputs,12 ADC inputs and 4 scalers) has been whiteout into the data file. The collected files has been transfered from the disk of the PC, running under "Windows-98", to the Linux PC for a further analysis by means of PAW.

1 Detector testing under cosmic rays and radiation source.

The assembly of 3 identical counters shown in Fig.5 has been used for various test with ionization source and cosmic particles. We have collected events at two HV settings:"high" and "low". The individual PMTs voltage has

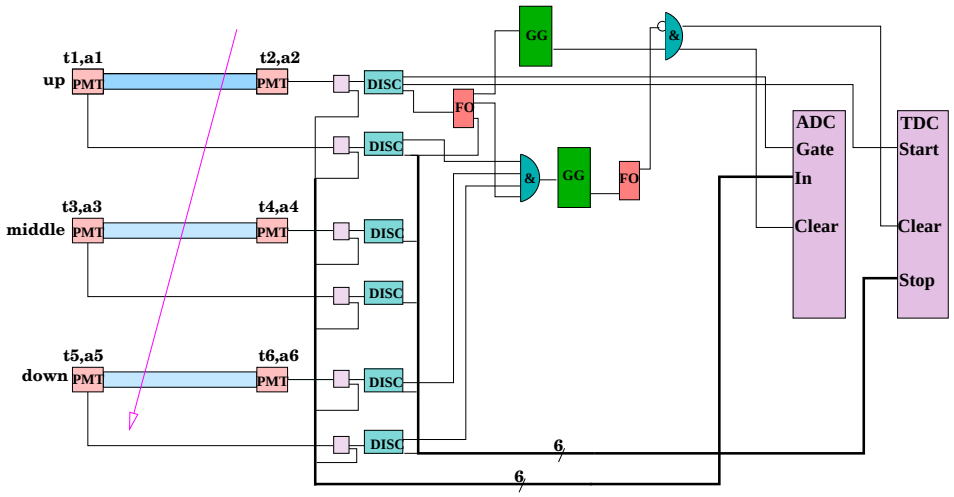

Figure 6: Experimental setup of 3 counters and electronic circuit diagram.

been adjusted for about equal gains. In order to set the appropriate HV we placed the ^{90}Sr source in the middle of the counter and observed the signals from both ends. The HV was chosen from the condition to see in the scope the mean amplitude of about 260mV("low") or 450mV("high") from both PMTs.

The counting rate with cosmic rays was of about 0.5 events per second. Therefore, in order to obtain data for the analysis we accumulated events during several days. The data taking period with the radiation source is of about 1min.

The data had been collected at different conditions both on cosmic rays and under the radiation source.

2 Methods and results.

We determined σ_{PMT} with three different methods, utilizing one, two and three identical counters, respectively. These methods and their results are presented in the following paragraphs.

Coordinate method. In the end of 2003 we have developed a new method for measuring the PMT resolution. The so called "coordinate method" is based on the simple relation between the light flash coordinate x and arrival

times, t_l and t_r, of signals from two PMTs, located at the ends of an extended scintillator:

$$t_x = t_l - t_r = \frac{2x}{c_s} + const, \tag{1}$$

where x is the coordinate of the light flash, t_x is the value digitized by TDC, c_s is the effective speed of light in scintillating media, l is the length of scintillator; *const* accounts for all kinds of propagation delays.

The standard deviation of t_x relates to the individual left and right PMT resolutions as

$$\langle(\delta t_x)^2\rangle = \langle(\delta t_l)^2\rangle + \langle(\delta t_r)^2\rangle + \langle(\delta t_{TDC})^2\rangle + \left(\frac{2x}{c_s}\right)^2 \langle(\delta x)^2\rangle \tag{2}$$

where $\langle(\delta t_{l,r})^2\rangle$ are the timing standard deviations for left or right PMTs; we assume that $\langle(\delta t_l)^2\rangle = \langle(\delta t_l)^2\rangle = \sigma^2_{PMT}$, $\langle(\delta t_{TDC})^2\rangle$ is the intrinsic resolution of the TDC, $\langle(\delta x)^2\rangle$ represents the size of the radiation source.

The ionization with known coordinate may be provided with a narrow beam of β-particles from the ionization source. Thus, from this formula one can determine the single PMT resolution as

$$\sigma_{PMT} = \frac{1}{\sqrt{2}}\sqrt{\langle(\delta t_x)^2\rangle - \langle(\delta t_{TDC})^2\rangle - \left(\frac{2x}{c_s}\right)^2 \langle(\delta x)^2\rangle} \tag{3}$$

We illustrate the coordinate method in Fig.7, in which we show the images of the source in the x-coordinate scale. These images were obtain "off-line" in two energy intervals of β-particles via Eq.(1). The peaks at about zero indicate the ionization source, placed in the middle of the counter. The wide distribution within $\pm 25cm$ is the manifestation of cosmic particles.

Measurements of the β-beam size. We note that the beam spot size of $5mm$ along the scintillator translates into the spread of the signal arrival time of about $30ps$. Therefore, this essential parameter has to be measured. In our tests we used the ^{90}Sr source with $E^{max}_{\beta} = 2.28MeV$. Its beam spot size was measured in following way.

The ionization source had been displaced across the scintillating counter with a step of 1mm, as shown in Fig.8. For each source position the counting rate had been recorded. The counting rate vs source displacement is shown in Fig.8,A). Each point on this plot displays the integrated beam profile.

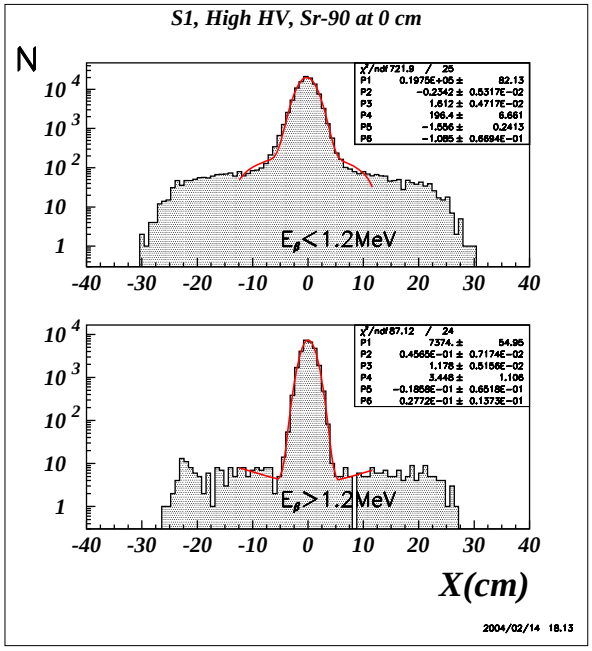

Figure 7: The "β-ray" images of ^{90}Sr source in two energy intervals of β-particles. Top panel - $E_\beta < 1.2MeV$. Bottom panel- $E_\beta > 1.2MeV$.

It has been integrated over the counting area of the scintillator shown as a dark spot in Fig.8. The size of this area varies with the displacement of the source. In order to obtain the profile of the beam, we have differentiated the curve in Fig.8,A). The resulting beam profile is shown in Fig.8,B). The fitted standard deviation was found to be $2.9 \pm 0.25mm$. This value has been used for estimating the PMT resolution via Eq.(5).

TDC calibration. The second important value, contributing to the t_x spectra, is the intrinsic resolution of the TDC. In order to measure the TDC intrinsic resolution and to calibrate the TDC scale, as well, we used random signals from one of PMTs as "start" signal. The initially same signal, taken from the fan-out, has been delayed with a step of $4ns$ and used as a "stop". The resulting spectrum is shown in Fig.9. From the mean values of two peaks one can evaluate the width of the TDC channel. he averaged value of $\langle \tau_{TDC} \rangle$ was found to be of $46.5ps$. The averaged calibrating peak RMS yields of $0.3ch$. From our earlier calibration we obtained $\langle \tau_{TDC} \rangle = 45.4ps$. Later we realized that this previously measured value may be underestimated due to systematic errors. The systematics comes from both the delay and TDC. The integral nonlinearity of LeCroy 2228A TDC is specified as ± 2 counts, while

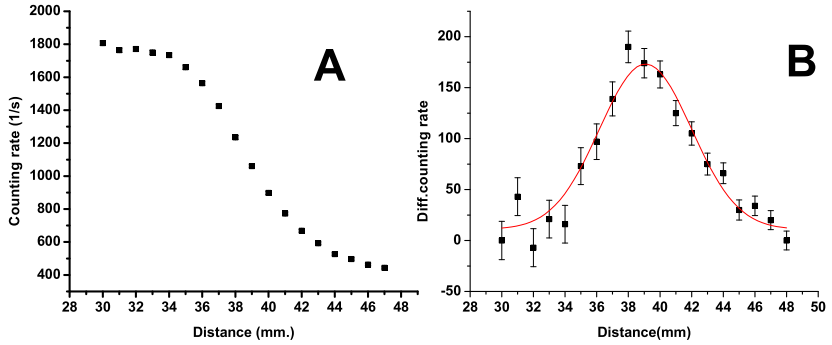

Figure 8: Measuring of the beam profile with ionization source. A)-integrated counting rate vs distance. B)-differential counting rate, i.e.beam profile.$\sigma = 2.9 \pm 0.25mm$.

the differential nonlinearity(i.e. variations of τ^i_{TDC} with channel number i) may be as high as $\pm 30\%$ during long measuruments. The time interval of t_x, corresponding to the full width of the scintillator, is of about $8ns(\approx 170ch)$. Thus, the systematic error may be estimated as $\pm 2/170 = \pm 1.2\%$. Together with the uncertainty of the delay of about1% , it may be an excuse for a systematic error of about $\pm 2.2\%$ in $\langle \tau_{TDC} \rangle$. Therefore, we admit that previously defined width of the TDC channel may be about of 4.4% wide . Therefore, we plan to make a more accurate and permanent calibration of our TDCs in future measurements with the Laser Calibration System.

PMT resolution from on-line measurements. The application of this method for the "on-line " measurements is demonstrated in Fig.11. The on-line t_x spectrum, shown in this figure, was digitized by TDC at three positions of the ionization source separated by $15cm$ with the energy threshold of about $1.4MeV$. Peaks were fitted by a Gaussian. Resulting width pf peaks is shown in this figure. Note, that "width " is the specific parameter of the "Origin-7" software. These value is twice as much of the standard deviations of a

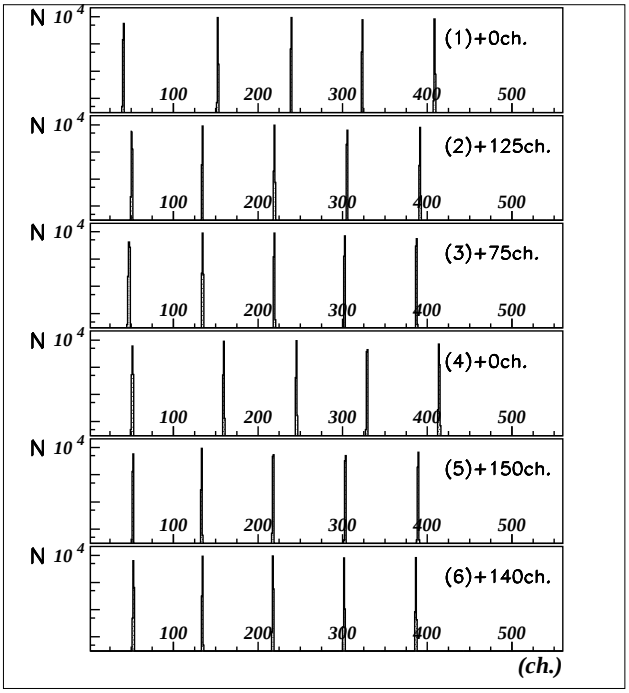

Figure 9: TDC calibration via known delay.

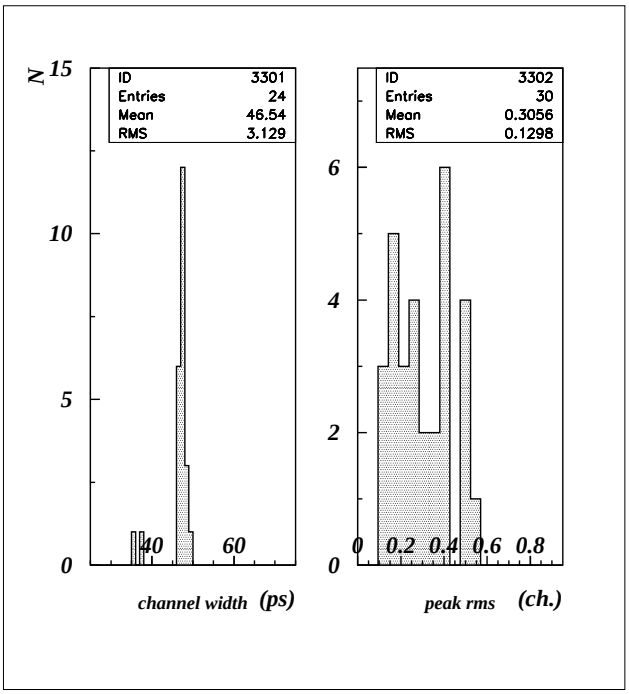

Figure 10: Left: the statistics of the TDC channel widths between calibration peaks. Right: the statistics of RMS values for calibrating peaks.

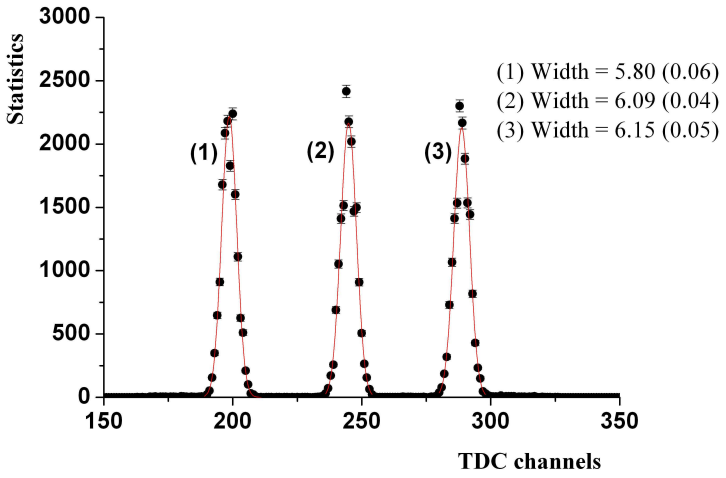

Figure 11: Images of ^{90}Sr in TDC scale. Spectrum was taken at three locations of the source separated by $15cm$. The shown "widths " are twice as much of the standard deviation of the corresponding Gaussian.

corresponding Gaussian.

The single PMT resolution has been determined via Eq.3 taking into account the finite beam spot size (0.3cm) and intrinsic resolution of TDC(1ch.). The value of $\sqrt{\langle(\delta t_x)^2\rangle}$ has been determined as a half of the peak width, displayed in this figure, multiplied by a the width of the TDC channel. After the correction for the finite beam size we obtained the value of σ_{PMT}=$94 \pm 10 ps$. The error of this value was roughly estimated from several fits in different intervals around the peak.

Energy dependence and extrapolation to MIPs. From the off-line analysis of the data files accumulated with the radiation source we have determined the dependence of the PMT resolution upon the energy of β-particles. Typical outcomes of such studies are shown in Fig.12,13. Each of these two figures contain plots for one of two source locations: $+15cm$ and $-15cm$ respectively. Below we explain the contents of each panel refered to as "(raw-column)".

- (1-1).Energy(E) spectra of β-particles. The energy of β-particles has been determined as

$$E = k\sqrt{(a_l - p_l)(a_r - p_r)} \tag{4}$$

  where $a_{l,r}$ and $p_{l,r}$ are the amplitudes and pedestals from ADCs corresponding to left or right sides of the counter; k is the calibrating factor, which been determined from the fit of the β-spectrum by the formula

$$n(\varepsilon) = G(\sigma, \mu)(\varepsilon)\sqrt{(\varepsilon^2 - 1)}(\varepsilon_0 - \varepsilon)^2 \tag{5}$$

  where $\varepsilon = E/m_e c^2$, $n(\varepsilon)$ is the number of events with specified ε, ε_0=$2.28 MeV/m_e c^2$ specifies the upper limit of the β-spectrum, G is a Gaussian.

- (2-1).The distribution of events over the longitudinal coordinate X defined via Eq.1 in ns. The peak at zero is the image of the source.

  Scatter plots X vs E has been also created for both locations. The energy slices $100keV$ wide has been fitted then by a Gaussian. Thus, the dependence $\sigma_X(E)$ has been measured. It is shown in the next panel.

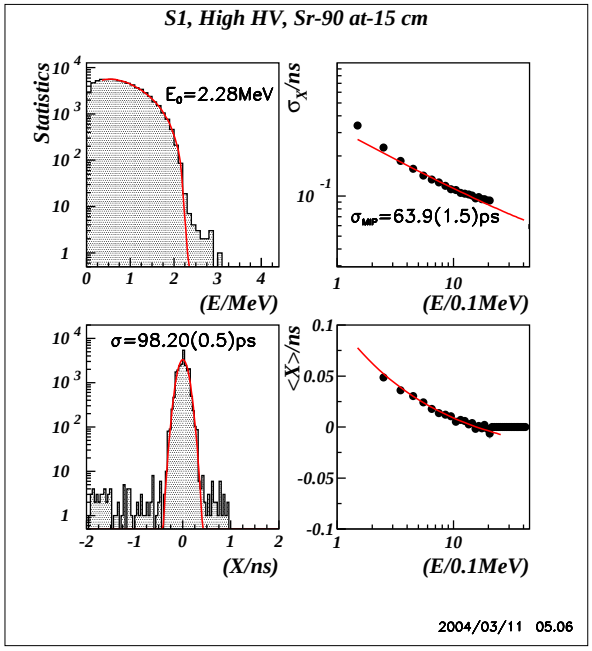

Figure 12: Coordinate method for "up" counter($S1$) at ^{90}Sr locations $-15cm$. Panel: (1-1) - energy (E) spectrum of β-particles ; (2-1) - coordinate(X) spectrum of β-particles; (1-2) - σ_X of the peak vs β-particle energy(E); (2-2) - $\langle X \rangle$ of the peak vs β-particle energy(E). The position of peak on X-scale was adjusted to zero for convenience.

- (1-2).Energy dependences $\sigma_X(E)$. As one can see from these plots σ_X varies as $1/\sqrt{E}$. Obviously this behavior is due to the increas of the signal-to-noise ratio. Extrapolating $\sigma_X(E)$ to the energy deposit of minimum ionizing particles in $2.3cm$ thick scintillator $E_{MIP} = 4.4MeV$ one can predict, roughly, the effective value of a PMT resolution for MIPs(σ_{MIP}). Thus obtained resolution is displayed on both panels. Such studies were performed for all 3 counters at 3 locations of the source. The mean over nine values was found to be of $61.8 \pm 1ps$.

- (2-2).The energy dependence of the center of the ^{90}Sr image $\langle X \rangle(E)$. The attention should be payed to the fact that there are obviously opposite displacements of both source images with decreasing energy.

Advantages of the coordinate method. The coordinate method has several important advantages. Firstly, it requires only one counter instrumented with two identical PMTs. Secondly, the data taking and data analysis

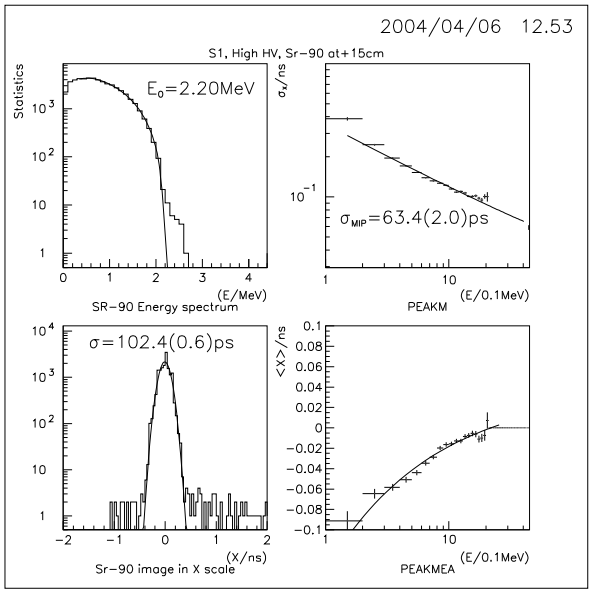

Figure 13: Coordinate method for the "up" counter($S1$) at ^{90}Sr locations $+15cm$. Panels on both pictures display: (1-1) - energy (E) spectrum of β-particles ; (2-1) - coordinate(X) spectrum of β-particles; (1-2) - σ_X of the peak vs β-particle energy(E); (2-2) - $\langle X \rangle$ of the peak vs β-particle energy(E). The position of peak on X-scale was adjusted to zero for convenience.

up to the final value takes only several minutes. Finally, this method is free of the systematics related to the coordinate dependence of signal's timing, since the ionization is localized in known narrow area of $\pm 0.3cm$. Moreover, the coordinate method may be used for studies of the coordinate dependent systematics. The last may be measuring directly at different locations of the ionizing source. This method may be also used as an express "on-line" method for studies of the PMT resolution in different environments.

Since the yielding value of σ_{PMT} is antiproportional to $\sqrt{E_\beta}$ the "on-line" result of this method will be notisably better if the ionization source $106Ru(E_\beta^{max} = 3.541MeV)$ will be implemented.

3 Cosmic ray method.

The cosmic ray method is based on the precise measurement of the time-of-flight of cosmic particles. Two counters, for instance "up" and "down", are enough for this method. The advanced modification of this method requires three identical counters with additional "middle"-counter. Both methods are available for measuring of the PMT resolution with our setup,

These methods utilize the following common relations. The time instants of the light flashes $t_{u,m,d}$ in the "up-", "middle-" and "down"-counters respectively are defined as:

$$t_u = \frac{1}{2}(t_1 + t_2); t_m = \frac{1}{2}(t_3 + t_5); t_d = \frac{1}{2}(t_5 + t_6), \tag{6}$$

where $t_{i=1,\ldots,6}$ are the corresponding TDC readout values. We note that values $t_{u,m,d}$ are expected to be independent upon the coordinates along scintillators. The longitudinal coordinates of the light flashes $x_{u,s}$ may be determined as

$$x_u = \frac{1}{2}(t_1 - t_2); x_m = \frac{1}{2}(t_3 - t_5); x_d = \frac{1}{2}(t_5 - t_6). \tag{7}$$

For illustration of the detector performance in Fig.14 we show the measured x-coordinate distributions.

We note that values $t_{u,m,d}$ are expected to be independent upon the coordinates along scintillators. Below we consider two methods in details and present our preliminary results.

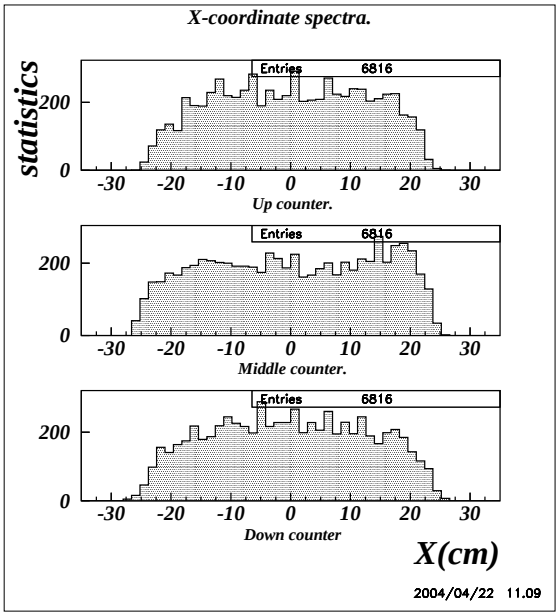

Figure 14: Coordinate distribution of cosmic tracks.

Method of two counters. With this method we measure TOF distribution between two identical "up-" and "down-" counters. We assume that all four PMTs have equal timing resolution.

The value of TOF depends upon both the velocity of the cosmic particle and its range between counters. The last is due to the fact that the trajectory is not exactly vertical and its inclination angle vary from event to event. The range of the cosmic particle between counters(l_{of}) may be determined as

$$l_{of} = \sqrt{((x_u - x_d)^2 + d^2)}, \tag{8}$$

where d is the distance between two counters($15cm$). From Eqs.(6,7) the time of flight between two counters, t_{of} yields:

$$t_{of} = \frac{1}{2}(t_1 + t_2 - t_5 - t_6) - c^{-1}\sqrt{((x_u - x_d)^2 + d^2)}, \tag{9}$$

where c is the speed of relativistic cosmic particle(speed of light). One can see from the Eq.(9) that at $(x_u - x_d) \approx 0$

$$\langle(\delta t_{of})^2\rangle \approx \sigma^2_{PMT} \tag{10}$$

Corresponding cosmic tracks has to be almost vertical in order to satisfy the mentioned above condition. The time-of-flight spectrum for "vertical" tracks in the central region of both counters is shown in Fig.16. The resulting from this distribution resolution of PMT was found to be of $\sigma_{PMT} = 57 \pm 2ps$.

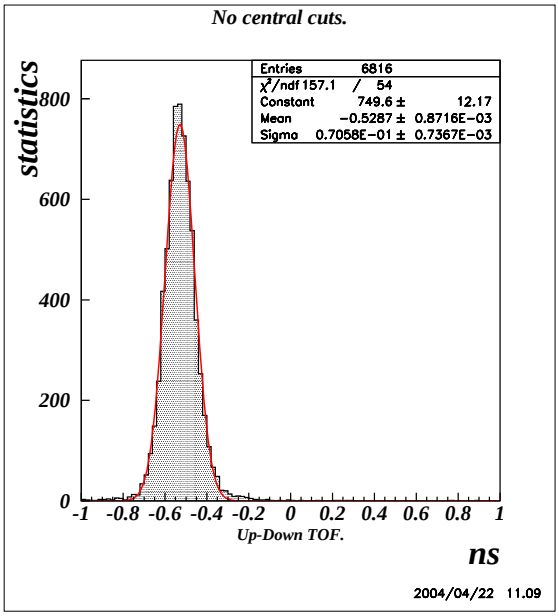

Figure 15: TOF distribution between two counters. No geometry cuts on cosmic tracks were applied. Sigma=71±1ps.

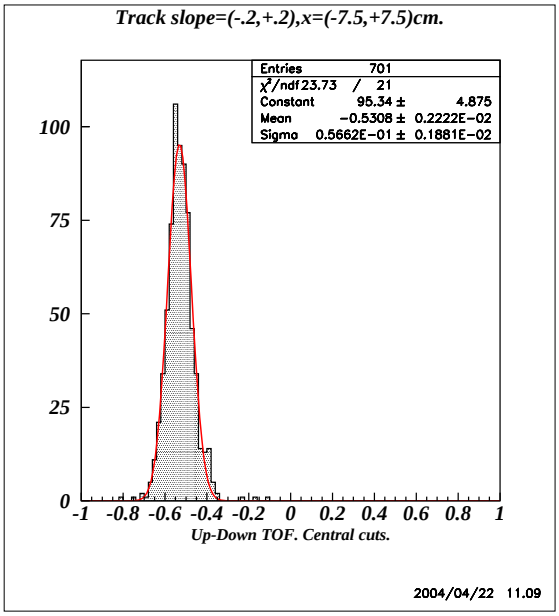

Figure 16: Time-of-flight distribution for cosmic tracks within $15cm$ wide area($\pm 7.5cm$) of both counters.Sigma=57±2ps.

For comparison we show the time-of-flight spectrum for all tracks obtained with no cuts on tracks parameters. The outcome for the resolution is worse in this case ($\sigma = 71 \pm 1ps$). There are at least two possible reason for that. Firstly, the coordinate dependence at $(x_u - x_d) \gg 0$ of the range between counters (Eq.9) does introduce the additional term to smearing of TOF. Secondly, there is a coordinate dependent systematics in measuring PMT-timings. We are going to study this systematics in further tests.

Method of three counters. If the cosmic particle of constant velocity hits three parallel and equidistant counters, then the following relation between ideally measured $t_{u,m,d}$ holds:

$$t_{umd} = t_m - \frac{1}{2}(t_u + t_d) = 0, \tag{11}$$

This relation obviously follows from the geometry of interaction. However, since the values $t_{u,m,d}$ are smeared by the time resolution, the value t_{umd} has to be smeared around zero, as well. Hence, the method is based on the statistical analysis of the residuals of Eq.(11):

$$\delta(t_{umd}) = \frac{1}{4}(\delta t_1 + \delta t_2) - \frac{1}{2}(\delta t_3 + \delta t_4) + \frac{1}{4}(\delta t_5 + \delta t_6) \tag{12}$$

It is important to notice that according to Eq.(12)

$$\langle(\delta t_{umd})^2\rangle = \frac{3}{4}\langle(\delta t_i)^2\rangle = \frac{3}{4}\sigma^2_{PMT} \tag{13}$$

where $i = 1, ..., 6$(we assume again that all PMTs have identical timing properties). Therefore, σ_{PMT} has to be $\sqrt{\frac{4}{3}}$ times of the measured standard deviation of t_{umd}. This is unlike the method of two counters (see Eq.10).

The measured distributions of $\delta(t_{umd})$ are shown in Fig.17.

The resulting value of single PMT resolution for the central region yields $\sigma_{PMT} = 96.1 \pm 3.2ps$. The overall resolution, with no cuts, yields $\sigma_{PMT} = 108.2 \pm 1.4ps$. The difference between two values may be accounted by a coordinate dependent systematics. The σ_{PMT} resulting from this method is obviously worse than from two counters method. The reason, perhaps , is that threshold discriminators has been used for the "middle"-counter. These discriminators has a worse time resolution, as we have concluded from the two counter method applied to the "up-middle" and "middle-down" pairs. Therefore, we plan to replace these discriminators in future.

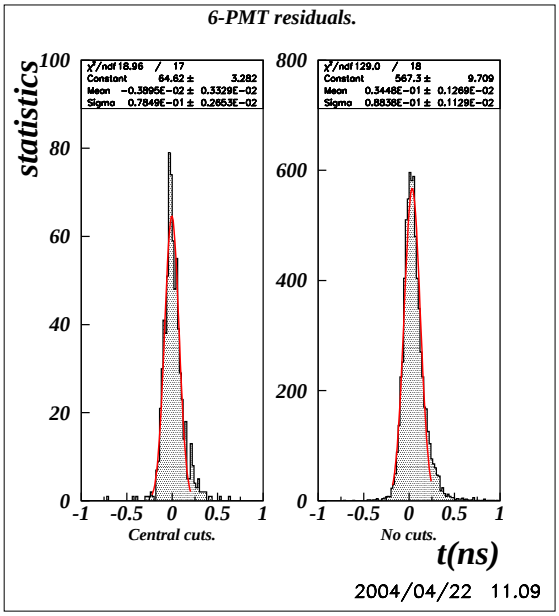

Figure 17: Distribution of residuals for the method of three counters. Left panel: horizontal scale - residuals of Eq.12, central cut. Right panel: same,but no cuts.

Long term stability. With the method of 3 counters we can investigated the long term stability of the timing system. Such study is illustrated in Fig.18.

The residuals of t_{umd} on the top panel show instable behavior. From the period of variations we have concluded that instability relates to our air-conditioner, which automatically change its operation mode with a similar period. From the extended study we have found that it influence the signal from the right side of the counter S2 ("middle" counter).

4 Summary and discussion.

We have discussed all the details of PMT resolution measurement and many related spectra has been shown, as well. The values of σ_{PMT} resulting from different methods are shown in the Table.1. We consider these results as very preliminary, since we are permanently developing our "off-line" software.

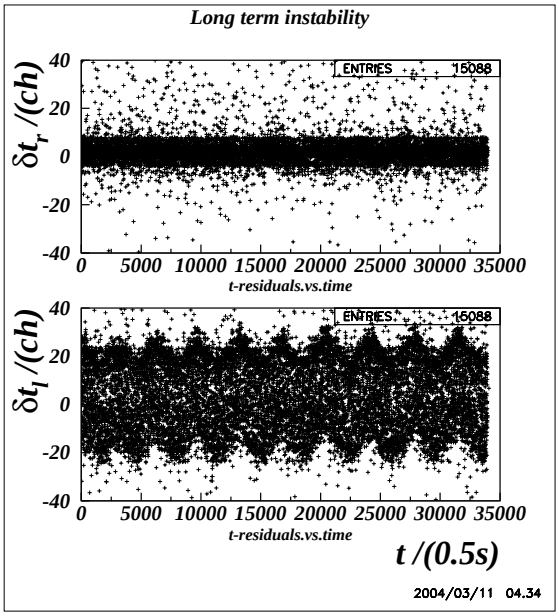

Figure 18: The indicative of the timing instability. Top panel:stable behavior ot the residuals. Bottom panel: oscillating residuals; the period is of about 1 hour.

Method	Acceptance	Particles	ΔE	σ_{PMT}
x-coordinate, 1 counter	$x \pm 2.8mm$	$\beta, (^{90}Sr)$	$E_\beta < 2.28MeV$	$94 \pm 10ps$
x-coordinate, extrapolation	$x \pm 2.8mm$	–	*extrapolated* $\approx 4.4MeV$	$62 \pm 1ps$
2 counter tracking	$0 \pm 7.5cm$	cosmic	$\approx 4.4MeV$	$57 \pm 2ps$
2 counter tracking	$0 \pm 25cm$	-	-	$71 \pm 1ps$
3 counter tracking	$0 \pm 7.5cm$	-	-	$96 \pm 3ps$
3 counter tracking	$0 \pm 25cm$	-	-	$108 \pm 2ps$

Table 1: PMT resolution(standard deviation) from different methods.

The errors shown in this table are yielded by the fitting procedures. The error for the on-line x-coordinate method has been estimated from several fits in different fitting intervals. This error is higher than others. The reason is that the shape of the "on-line" peak is not a perfect Gaussian, first of all, due to the differential nonlinearity of TDC. In the off-line measurements this

effect is not seen because of the smearing over the large number of channels.

The systematic error has been discussed above with respect to TDC calibration. We declare our possible systematic error to be of about $+4.4\%$ to the shown values.

The result from the local x-coordinate method with extrapolation is very close to that of the method of 2 counter tracking, especially in the narrow area $0 \pm 7.5cm$. This method looks very promising as an express method.

The result of the 2 counter method in the wide area $0 \pm 25cm$ is worse then in the narrow $0 \pm 7.5cm$. This may be explained by the existing coordinate dependent systematics of the PMT timing.

The σ_{PMT} from the tracking method with 3 counters is worse, because the "middle" counter has been involved into this measurements. This counter is instrumented with worse discriminators. We also observe a long term instability in one of its timing channels.

The results shown in Table1 were obtained with the prototype, which has no light guides. The actual conditions for the light collection will be significantly worse. Therefore, we consider these values as the most optimistic limit of σ_{PMT}. However, we believe that we can improve the outcome from these methods via accurate accounting for the coordinate dependent systematics and improving the performance of the apparatus.

Year 2004

For the Year 2004 we plan to perform rigorous tests of PMT resolution using the setup of three identical counters.

Studies. We are going to compare different designs of a light guide and different types of PMTs, as well.

We'll study coordinate dependent systematics of PMTs timing by means of both radiation source (^{106}Ru,^{90}Sr) and cosmic ray tests.

Also we intend to study the HV dependence of resolution and dependence of resolution upon the length of signal cables, as well.

We plan to implement the laser calibration system in order to avoid the long term instabilities of measuring values.

We plan to migrate from CAMAC to VME-based Data Acquisition System. Our final goal is to test the performance of the set of 3 prototypes at

the accelerator, in real experimental environments.

The main goal is to achieve the time resolution of a single PMT as close as possible to the desired value of $50ps$ under the accelerator environments. This will be done with three counters with long light guides shown in Fig.2.

Equipments and DAQ. With this purpose for the Year 2004 we plan the following.

- to fabricate six long light guides;
- to fabricate three detectors with 1m long light guides;
- to make a setup of 3 counters;
- to replace the CAMAC-based by the VME-based Data Acquisition System;
- to replace the threshold CAEN N413A discriminator by ORTEC-935 CFDs;
- to incorporate the laser calibration system into the setup and DAQ.